Proceedings of OMAE2005
24th International Conference on Offshore Mechanics and Arctic Engineering (OMAE 2005)
June 12-17, 2005, Halkidiki, Greece

OMAE2005-67303

ELASTO-PLASTIC BEHAVIOR AND BUCKLING ANALYSIS OF STEEL PIPELINES EXPOSED TO INTERNAL PRESSURE AND ADDITIONAL LOADS

Peter Schaumann [1] **Christian Keindorf** [1] **Henning Brüggemann** [2]

[1] Institute for Steel Construction, University Hannover
Appelstr. 9A, 30167 Hannover, Germany
phone: +49 511 762-3781
fax: +49 511 762-2991
schaumann@stahl.uni-hannover.de

[2] Dr.-Ing. Veenker Ingenieurgesellschaft mbH
Heiligengeiststr. 19, 30173 Hannover, Germany
phone: +49 511 28499-12
fax: +49 511 28499-99
henning.brueggemann@veenkergmbh.de

ABSTRACT

The currently valid worldwide standards allow for taking into consideration plastic deformations in order to achieve a higher degree of utilization. The maximum plastic strains, which can be allowed for steel pipes subjected to internal pressure and additional loads, are particularly interesting. In this paper results of investigations on the elasto-plastic bearing behavior of steel pipelines subjected to internal pressure and bending are presented. Four-point bending tests on eight steel pipes were carried out in order to make the buckling analysis in the elasto-plastic range possible. Finite-element-models were checked by test results for the application on buried pipelines. Taking into account bedding conditions of the pipeline in the soil was made possible. Furthermore, an analytical method based on the differential equation for beams with longitudinal tensile force and variable bending stiffness was developed. It is suitable to determine the elasto-plastic bearing capacity for internal pressure and bending. The collapse due to plastic shell buckling is considered by a limit criterion based on critical strains.

Keywords: pipeline; elasto-plastic; buckling; strain limit; analytical method; interaction pipe-soil

INTRODUCTION

The design of steel pipelines in Germany is based on an elastic stress analysis and the check against the permissible yield stress (DIN EN 1594). Principle of the analysis is to determine the stresses caused by internal pressure and additional loads during erection, operation and service life. To evaluate the biaxial state of stress the available stresses are summarized to the equivalent stress, which must not exceed the yield stress.

The currently valid worldwide standards allow the consideration of plastic deformations in order to reach a higher degree of utilization. In several standards and publications limit states exist for pipelines loaded by combinations of internal pressure and bending. This paper focusses on the question, which maximum plastic strains can be allowed for typical tubular steel under internal pressure and additional loads, bearing in mind the demands for load-capacity, integrity and safety of pipelines.

The aim of the research is to demonstrate the benefits of limit state design for high pressure pipelines based on the consideration of plastic strains and to add experimental and numerical data for the validation. Limit values satisfying the requirements for safety and economy have to be defined.

NOMENCLATURE

a	Ovalisation at $\theta = \pi/2$ and $\theta = 3\pi/2$
D	Outer diameter
D_{max}	Maximum measured diameter per pipe cross-section
D_{min}	Minimum measured diameter per pipe cross-section
E	Young's modulus
F	Reaction force
Δ_o	Initial out-of-roundness
$f_{u,k}$	Characteristic tensile strength
$f_{y,k}$	Characteristic yield strength
I	Moment of inertia of pipe cross-section

M	Bending moment
N	Axial tensile force
P	Internal Pressure
r_m	Average pipe radius
r´	Radius of ovalised pipe
t	Nominal wall thickness
u; u_k	Deformation, imposed deformation
$\dot{u}$	Deformation rate
w(x)	Deflection
ε_{el}	Elastic strain
ε_{pl}	Plastic strain
ε_{cr}	Critical strain
$\kappa(x)$	Curvature
ν_{el}	Poisson's ratio in elastic range
σ_L	Longitudinal stress
σ_Z; σ_D	Longitudinal stress (Z = tension, D=compression)
σ_Θ	Hoop stress
σ_v	Equivalent stress
σ_y	Yield strength
θ	Circumferential angle

SCALE MODEL TESTS

A series of scale model tests (D/t = 132) was carried out to investigate the elasto-plastic bearing behavior of steel pipelines exposed to internal pressure and additional imposed bending deformation. The test setup as shown in Fig. 1 was used for this purpose.

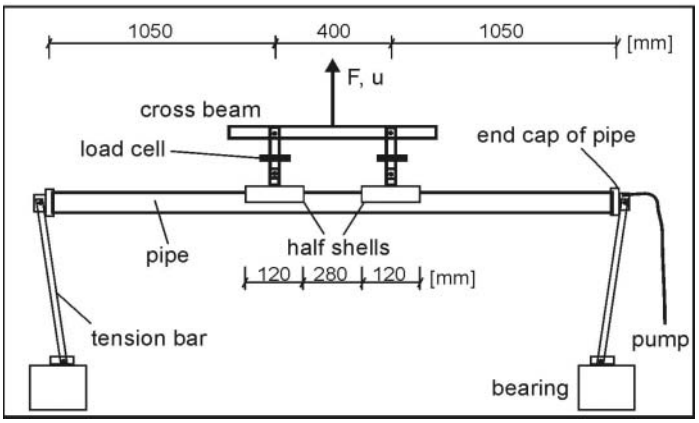

Figure 1: Test setup

In principle, it is a classical four-point bending test. In order to avoid local failure at the point of load application, a construction with steel half-shells was realized. The shells were glued to the tension side of the test pipes using a two-component epoxy resin adhesive. At these the test specimen is deformed in an upward direction. The ends of the pipes were simply supported. This test setup proved to be very well suited for the problem.

The test pipes consist of steel welded with a longitudinal seam having a yield strength of $f_{y,k}$ = 220 N/mm² and a tensile strength of $f_{u,k}$ = 300 N/mm². The outer diameter is D = 66.1 mm and the wall thickness is t = 0.5 mm. The real stress-strain curve was determined by tension tests.

The test pipes were produced and sponsored by a German company for pipe-systems. The origin of the pipes is a coil of coldformed steel with material number 1.0338 (EN 10027-2). Although the ratio D/t = 132 of these test pipes is not common for onshore pipelines the bearing behavior in elasto-plastic range and the effects of local buckling can also be observed for this thin walled pipe.

At first two tests were carried out to calibrate the test equipment and to determine the ideal distance for the points of load application. The subsequent test series was then undertaken using a distance of 400 mm between the points of load application (see Fig. 1). Maximum stress is expected in the centre of the pipe. The distance of the points of load application is greater than 4D, so that local effects may have died out. Table 1 gives an overview over the test program.

No.	Internal Pressure P [bar]	Imposed Deflection u_k [mm]	Remark
1	0	35.0	
2	15	76.0	
3	15	67.5	Pressure drop to P = 0 and rebuild-up to P = 15 bar
4	25	112.0	
5	25	110.0	Pressure drop to P = 0 and rebuild-up to P = 25 bar
6	5	43.0	
7	30	130.0	
8	30	182.0	Pressure drop to P = 0 and rebuild-up to P = 30 bar

Table 1: Test Program

The strains were evaluated using strain gauges attached to the test specimens. The internal pressure and the deformation of the pipe were recorded online by pressure sensors, inductive displacement transducers and potentiometers. The reaction force due to the imposed deflection was measured with two load cells. The internal pressure was applied via filling the pipes with water using a hand-operated pump. No leaks occurred in any of the tests carried out with partly marked local deformations and strains.

NUMERICAL SOLUTION VERSUS TEST RESULTS

The ovalisiation was measured at the pipes 1 to 8 before the tests beginning since this kind of imperfection has a great influence on the bearing behavior of tubular steels. The initial ovalisation was calculated using the formula:

$$\Delta_o = \frac{D_{max} - D_{min}}{D_{max} + D_{min}} \quad (1)$$

The average value was Δ_o = 1.0 %. The tests were carried out displacement-controlled, whereby pipe 1 was only subjected to bending and pipes 2 to 8 were subjected to bending and internal pressure (see Table 1). The horizontal and vertical deformations were measured using displacement transducers and potentiometers. Furthermore, load cells were located at both points of load application to measure the reaction forces

due to imposed deflection (see Fig. 1). In addition strain gauges were installed longitudinal and transverse to the pipes as well as a pressure gauge at one end cap of the pipe.

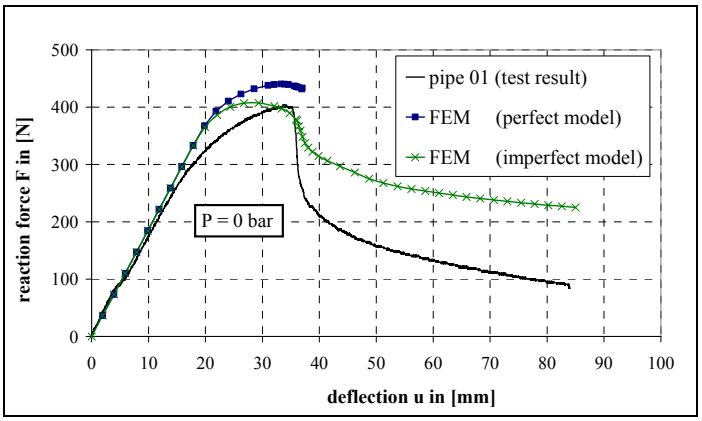

Figure 2: Force-Deflection curves for pipe 1

The curve of reaction force (average value of the two load cells) is represented as a function of the vertical imposed deflection in Fig. 2 for pipe 1 (P = 0 bar). These parameters were chosen for the comparison with numerical solutions because the values of F and u were directly measured during the test. The deflection u was measured in the middle of the pipe length. The reaction force rises linearly at the beginning of the test up to the elastic yield strength is reached. The transition to the elasto-plastic range can be recognized at a deflection of approx. u = 16 mm by the non-linear curve progression. A reason for the difference between measured values and calculated values above F = 300 N could be residual stresses due to the production processes (welding, cold forming). These residual stresses are not considered in FE-models. In the event of a further increase in the imposed deflection shell buckling is initiated by existing geometrical and material imperfections. After the onset of local buckling has occurred, the global deflection u will continue, but more and more energy of the applied bending energy will be accumulated in the local buckle. Shortly after reaching the maximum moment bearing capacity (u = 35 mm, F = 400 N) a geometrical collapse occurs, whereby the buckle springs inwards near the middle of the pipe. Simultaneously there is a significant drop in the force-deflection curve whereby a distinct reduction in the moment bearing capacity occurs.

Numerical simulations were made using the FE-program ANSYS for comparison with the test results. The model was generated with shell elements using symmetrical conditions. The real stress-strain curve of the tensile tests was implemented as material law.

The FE-calculations show a good agreement for the curves in the elastic range. The calculation with the perfect model achieves a maximum force of F = 440 N and ends with a deflection of u = 37 mm. For the calculation with imperfections, at first the buckling mode has to be selected, which qualitatively shows the deformation pattern of the test. This is done by a buckling analysis. Quantitative values of the imperfections are based on the measured values of ovalisation (Δ_o). The force-deflection curve of the model with imperfections has at u = 27 mm a maximum force of F = 407 N, which declines at u = 35 mm. Unlike to the perfect model this force-deflection curve extends right into the softening region, but the decline in force, however, can not be seen so clearly in comparison to test pipe 1.

The buckle shapes of test pipe 1 and of the FE-calculation with imperfect model are compared in Fig. 3. The start of buckling was located on the compression side near midspan of the pipe. It can be recognized that the position and form of the buckles agree very well with the test result.

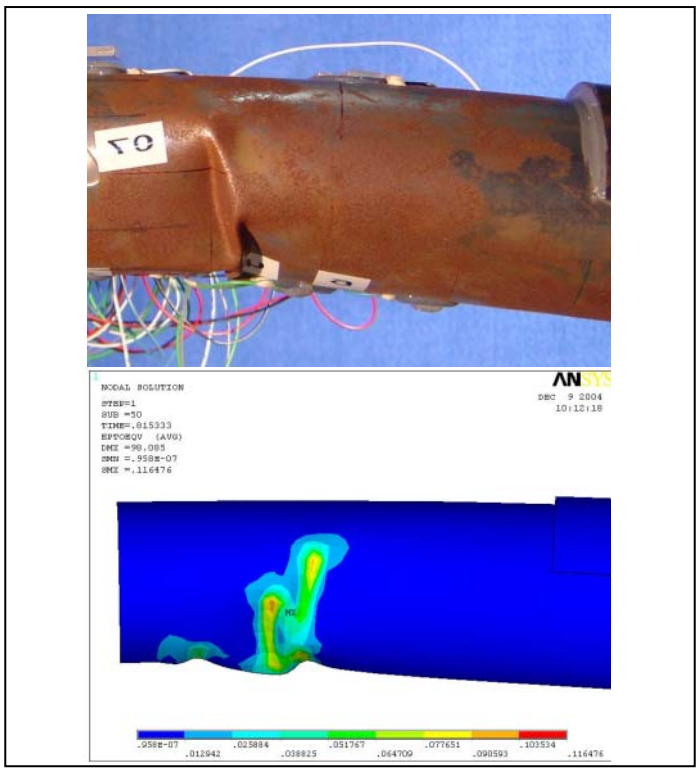

Figure 3: Comparison of buckling forms for pipe 1

In case of pipe 2 an internal pressure of P = 15 bar was applied via filling the pipe with water using a hand-operated pump. The ratio of the hoop stress to the yield strength was $\sigma_\Theta / \sigma_y = 0.45$. Subsequently the imposed deflection was increased, whereas the internal pressure was kept constant. At u = 45 mm, where pipe 1 already showed failure due to local buckling, the imposed deflection was stopped, to inspect the surface of the pipe. No significant buckling was discovered. Only at approx. u = 60 mm several ripples could be recognized along the pipe axis on the compression side. At u = 76 mm the deformation of a single ripple (wave) increased and a buckle became more significant, and bulged outwards due to the stabilization caused by internal pressure. At the same time a decrease for the reaction force could be observed at the load cells.

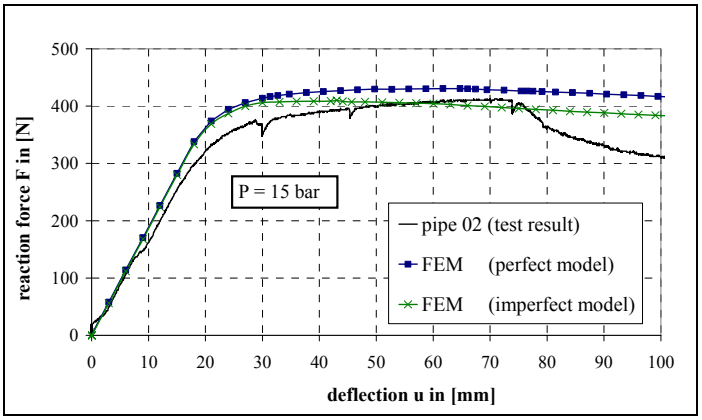

Figure 4: Force-Deflection curves for pipe 2

In comparison to pipe 1 greater deflections could be achieved without stability failure both in the test as well as in the simulation due to the increased buckling resistance caused by the internal pressure. The numerical simulation with the perfect model reaches a maximum value of F = 430 N at u = 62 mm (see Fig. 4). In the case of the calculation with imperfections the maximum reaction force is F = 407 N. Contrary to the test result, both numerical force-deflection curves show no significant drop in force where the single buckle occurred in the test. The reason for this difference can be explained with the slightly pressure reduction due to the increase of volume. Because the pressure reduces during the test the increased buckling resistance is decreased again and leads to local buckling. If this effect of a slightly pressure reduction during the imposed deflection is taken into account in the FE-simulation, a single buckle and also a drop in force could be observed like in the test.

The buckling shapes of test pipe 2 and the FE-calculation with imperfections are compared in Fig. 5. Buckling begins on the compression side near the middle of the pipe. It can be seen that the position and form of the buckles correspond very well. The ripples that are built up along the pipe axis in the prebuckling phase are also visible in the FE-simulation. In comparison to the test without internal pressure (pipe 1) the buckling behavior in the case of tests with internal pressure (pipes 2 to 8) is fundamentally different, because the hoop stresses due to internal pressure counteract the ovalising forces due to bending and so the buckling occurs for greater imposed deformations. The buckling figures under internal pressure are characterized by the establishment of a single buckle which develops outwards in a relatively narrow area with regard to the longitudinal direction of the pipe. The smoothing effect of the internal pressure on the imperfections leads to a further stabilisation of the tubular steel.

The scenario of a pressure drop was investigated at the pipe 3 in the elasto-plastic range. At first the pipe was deformed under an internal pressure of P = 15 bar up to a vertical deflection of u = 49 mm. After that the pipe was unloaded from P = 15 to 1 bar, while the imposed deformation was kept constant. The pipe cross-section remained stable thereby and no local buckling occurred. Only the reaction forces dropped back to the load level in relation to the actual static yield limit.

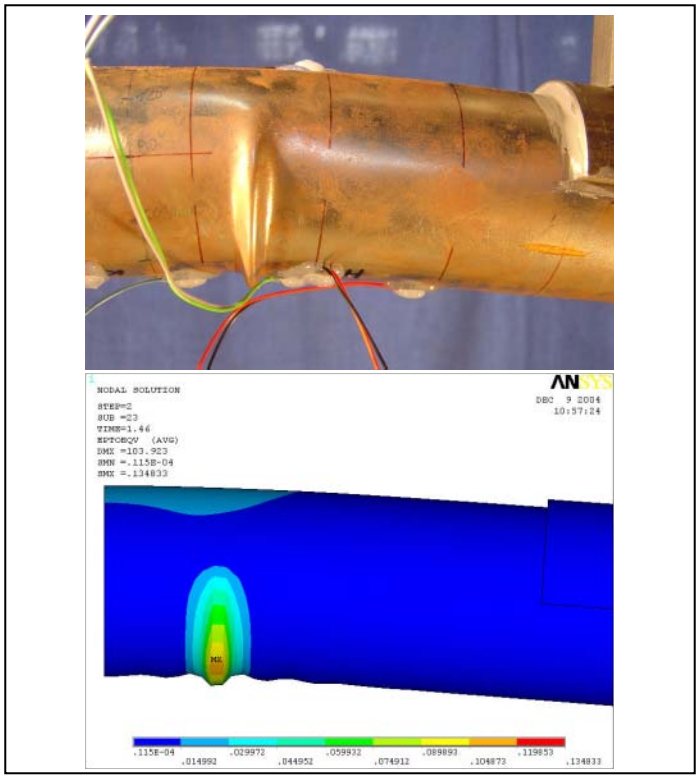

Figure 5: Comparison of buckling forms for pipe 2

After renewed pressure build-up to P = 15 bar the imposed deformation was increased further. At u = 67.5 mm the internal pressure was again reduced to 1 bar for the second time, whereby the pipe still remained stable and no buckling occurred. Only when the deflection u was further increased without pressure buckling failure immediately occurred in the compression zone. The form of buckling resembled that of the pipe 1 without internal pressure.

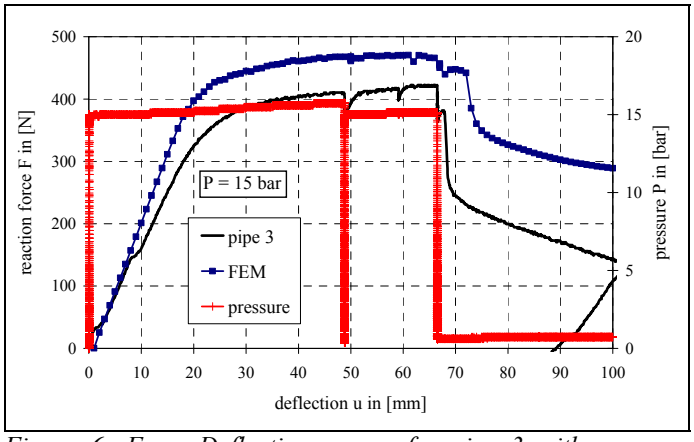

Figure 6: Force-Deflection curves for pipe 3 with pressure drop

This elasto-plastic bearing behavior could be confirmed with an FE-calculation, where a pressure drop at u = 49 mm and u = 67.5 mm was simulated. At both stop positions the pipe remained stable. Only in the case of a further increase without internal pressure a sudden buckle failure occurred similar to that in the case of the tested pipe 3. This phenomenon could be repeated using tests with the pipes 5 and 8 for different internal

pressures. From this it can be concluded that during a further increase of imposed deformations ($\dot{u} > 0$) there must be an internal pressure but this is not necessary for the stability if the deformation is kept constant ($\dot{u} = 0$). A further increase of deformations must not occur in pressureless conditions, since the supporting effect of internal pressure during development of further plastic strain increments is missing.

Furthermore, a gradual pressure reduction due to the increase in the volume of the pipes could be observed in the elasto-plastic range. This led to a gradual increase in the reaction forces, because assuming the Mises flow-hypothesis and a biaxial stress state a greater longitudinal stress (bending) due to the drop in the hoop stress (internal pressure) could be allowed considering the actual equivalent stress (see Eq. 2).

$$\sigma_V = \sqrt{\sigma_L^{\,2} + \sigma_\Theta^{\,2} - \sigma_L \cdot \sigma_\Theta} \tag{2}$$

STRAIN-LIMITS OF SCALE MODEL TESTS

For the following analytical method a limit criterion based on the consideration of plastic strains is needed. Fig. 7 shows the critical strains of the tested pipes as a function of the internal pressure. The values for ε_{cr} originate from the strain gauges on the compression side for the longitudinal direction (axial direction) at the beginning of buckling. A good approximation to the experimental limit strain curve is provided by equation 4. But for a limit criterion in the analytical method the empirical equation 3 is used because the values calculated with equation 3 are more on the safety side for higher pressure ratios.

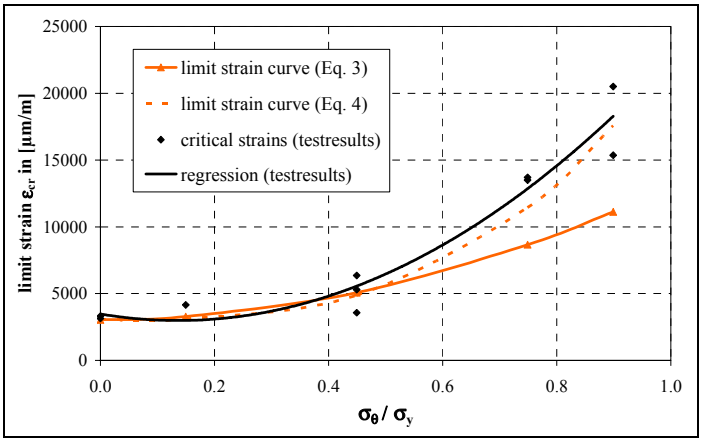

Figure 7: Critical strain limits for plastic shell buckling

$$\text{for } r_m/t = 65.6: \quad \varepsilon_{cr} = 0.2 \cdot \frac{t}{r_m} + 0.01 \cdot \left(\frac{\sigma_\Theta}{\sigma_y}\right)^2 \tag{3}$$

$$\varepsilon_{cr} = 0.2 \cdot \frac{t}{r_m} + 0.02 \cdot \left(\frac{\sigma_\Theta}{\sigma_y}\right)^3 \tag{4}$$

The first term of Eqs. 3 and 4 applies for the case of pure bending. The second term takes into account the increased buckling resistance due to internal pressure depending on the ratio of hoop stress to elastic yield strength. In literature [2, 8] for plastic shell buckling at pure bending a range for the critical buckling strains of

$$0.2 \cdot \frac{t}{r_m} < \varepsilon_{cr} < 0.4 \cdot \frac{t}{r_m} \tag{5}$$

is given. The increased buckling resistance due to internal pressure is taken into account according to a suggestion of Gresnigt [5] in semi-empirical equations (Eqs. 6 and 7). Based on test results values for buckling strains are indicated as dependent on pipe slenderness, Young's-modulus and internal pressure.

$$\text{If } \frac{t}{r'} > \frac{1}{60}: \quad \varepsilon_{cr} = 0.25 \cdot \frac{t}{r'} - 0.0025 + 3000 \cdot \left(\frac{P \cdot r}{E \cdot t}\right)^2 \cdot \frac{|P|}{P} \tag{6}$$

$$\text{If } \frac{t}{r'} \le \frac{1}{60}: \quad \varepsilon_{cr} = 0.1 \cdot \frac{t}{r'} + 3000 \cdot \left(\frac{P \cdot r}{E \cdot t}\right)^2 \cdot \frac{|P|}{P} \tag{7}$$

$$\text{with } r' = \frac{r}{1 - \frac{3a}{r}} \tag{8}$$

In comparison to the equations 3 and 4 Gresnigt [5] already gives design values and takes the ovalisation into account (Eq. 8).

ANALYTICAL SOLUTION VERSUS TEST RESULTS

The analytical method is based on differential equations (D.E.) for beams. The static system and loading conditions of the test pipes are represented in Fig. 8. It has to be taken into account that a longitudinal tensile force N is produced by the internal pressure on the pipe end caps. Because of that the general differential equation for beams with longitudinal tensile force (Eq. 9) is used for the analytical solution.

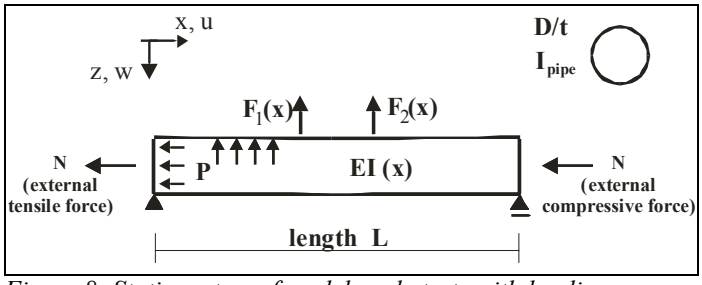

Figure 8: Static system of model-scale tests with loading

$$\left(EI \cdot w''(x)\right)'' + N \cdot w''(x) = F(x) \tag{9}$$

The solutions of the differential equation for w(x), ϕ(x), M(x) and Q(x) are calculated with trigonometrical constitutive functions as series expansions. No external forces N are applied (N = 0) in the test specimen. If $N \neq 0$ a case differentiation is to

be made. Furthermore, the bending stiffness is not constant in the elasto-plastic range, so that the general D.E. is used with EI(x). For the consideration of greater deformations the exact differential geometrical relationship between the deflection w(x) and the curvature κ(x) is implemented:

$$\kappa(x) = \frac{w''(x)}{\left(1 + w'(x)^2\right)^{3/2}} \tag{10}$$

The analytical method consists of an elastic and elasto-plastic part. The elasto-plastic calculation is carried out displacement-controlled and as an iterative method to determine the solutions for w(x), ϕ(x), M(x) and Q(x). The yield criterion according to v. Mises and the material law according to Prandtl-Reuss are chosen to consider the plasticity. The total axial strain is then the sum of the elastic strain and the plastic strain increments:

$$\varepsilon_{tot}(x) = \varepsilon_{el}(x) + \sum_{i=1}^{n} \varepsilon_{pl,i}(x) \tag{11}$$

The borders between elastic and plastic region are newly calculated in each iteration-step along the pipe axis (x-direction). The reduction of the bending stiffness EI(x) depending on the strain values on the tensile side max ε_Z and compression side max ε_D takes place in the elasto-plastic range. For this purpose the integral of the inner bending moment to the actual strain condition is calculated on the maximum stressed pipe cross-section.

$$\begin{aligned} M(x) &= 2 \cdot t \cdot r^2 \cdot \int \sigma_Z(\max\ \varepsilon_Z) \cdot \sin\theta \cdot d\theta \\ &+ 2 \cdot t \cdot r^2 \cdot \int \sigma_D(\max\ \varepsilon_D) \cdot \sin\theta \cdot d\theta \end{aligned} \tag{12}$$

Because the real stress-strain curve is implemented in the analytical method, the real stresses at each strain condition are determined ($\sigma_Z = f(\max\ \varepsilon_Z)$ and $\sigma_D = f(\max\ \varepsilon_D)$). As a consequence of this no simplifying assumptions (e.g. ideal-elastic, ideal-plastic) had to be implemented in the material law. The axial strain curves for the compression side at the midspan point of the pipe are compared in Figure 9. To compare the numerical solutions with the test results for the axial strain always the values for L/2 of the pipe were used. There is a very good agreement up to the elastic strain limit for the strain curve of pipe 1 with the numerically and analytically calculated strain curves. At approx. $\varepsilon_{cr} = 3250$ µm/m plastic shell buckling occurs on pipe 1 and after this the axial strain decreases (postbuckling range) because the strain gauges were not located at the local buckle. In the area of the local buckle strains will be much higher. FE-calculation with the perfect model shows very high strain values because the strain was taken from a point at midspan of the pipe where the local buckle occured.

The strain curve of the FE-calculation with imperfect model remains below the elastic strain limit. Using the analytical method according to Eq. 3 a critical strain value of $\varepsilon_{cr} = 3050$ µm/m is established. Furthermore it can be seen that applying the analytical method the nonlinear increase in the axial strain is determined within the elasto-plastic range.

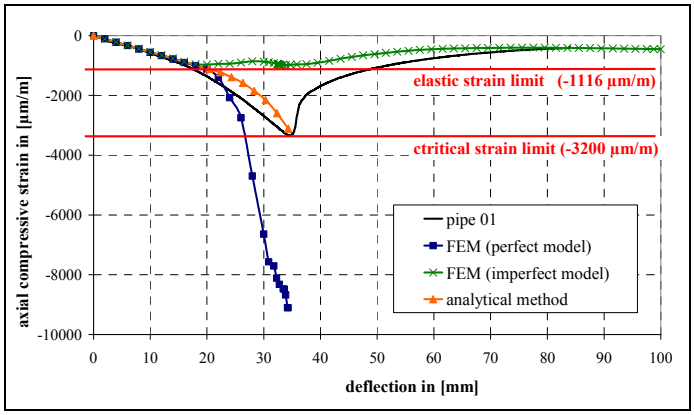

Figure 9: Comparison of the axial strain curves on the compression side

In order to take the biaxial stress status due to bending and internal pressure and assuming von Mises yield criterion (see Eq. 2) the following equation is derived (shear stresses will be negligible):

$$\sigma_v^{\ 2} = \sigma_L^{\ 2} + \sigma_\Theta^{\ 2} - \sigma_L \sigma_\Theta \tag{13}$$

The longitudinal stresses σ_Z and σ_D are formulated as a function of the hoop stress σ_Θ and the equivalent stress σ_y:

$$\sigma_L = \sigma_{Z;D} = \frac{\sigma_\Theta}{2} \pm \sigma_v \sqrt{1 - 0.75 \cdot \left(\frac{\sigma_\Theta}{\sigma_v}\right)^2} \tag{14}$$

To determine the maximum elastic strain increments in axial direction for the bending at the proportionality limit, the elastic strain increment of the longitudinal force as a result of cap pressure and traverse strain due to internal pressure are considered (N = positive for tensile force):

$$\varepsilon_{el,Z} = \frac{\sigma_Z}{E} - \frac{N}{EA} - \frac{P \cdot D}{4 \cdot t \cdot E} + \nu_{el} \cdot \frac{P \cdot D}{2 \cdot t \cdot E} \tag{15}$$

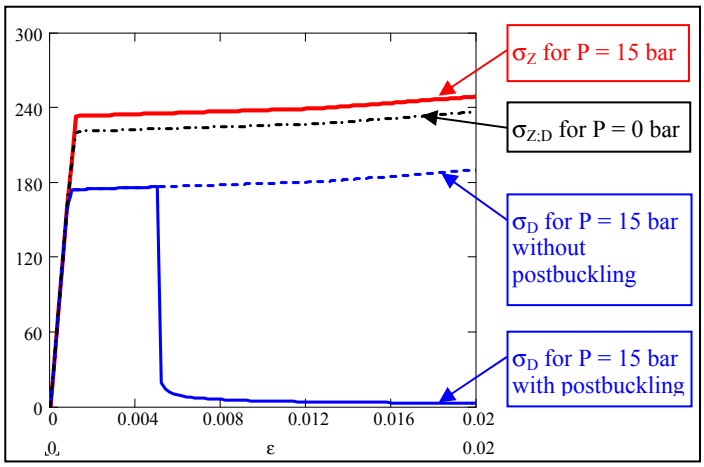

Figure 10: Stress-strain-curves for tensile and compressive range

The value $\varepsilon_{el,Z}$ is the maximum tensile strain, which can be provided for the bending of the pipe within the elastic range ($\varepsilon_{el,D}$ analog with Eq. 15 but with opposite sign).

The stress-strain curves of the tensile- and compressive side are identical for P = 0 bar. If P ≠ 0 bar, then according to the Mises yield criterion different values are determined for the yield strength in the tension and compression zone of the pipe (see Fig. 10).

The postbuckling behavior within the compression zone is approximated by an empirical formula (Eq. 16). It was derived with curve fitting for the tests carried out in this program. It has to be checked for other D/t ratio's.

The drop in stress for the compressive side is described depending on the ratio σ_Θ / σ_y and the critical strain value ε_{cr}. Because of this a simulated decrease in the reaction force occurs concerning the force-deflection curve. If the hoop stress is high, the reaction force will slightly drop within the postbuckling range. But if the hoop stress is low or zero, the reaction force decreases more distinct within the postbuckling range.

$$\text{postbuckling}(\varepsilon) = \frac{\sigma_D}{1 + 400 \cdot (\varepsilon - \varepsilon_{cr})^{\frac{\sigma_\Theta}{\sigma_y}}} \quad \text{for } (\varepsilon > \varepsilon_{cr}) \qquad (16)$$

The results of the analytical method and of the tests with P = 0 und 15 bar are compared in Figure 11. In the case of the analytical calculations the strain-based limit criterion according to Eq. 3 is applied. For the case without internal pressure (pipe 1) a significant drop occurs after the critical strain has been reached on the compressive side. The force-deflection curve of pipe 1 does not reach the maximum value of the analytical method, because the influence of imperfections is not taken into account by the analytical method. The imperfections decrease the load bearing capacity significantly in the unpressurized condition, so the force-deflection curve of pipe 1 is rather nonlinear.

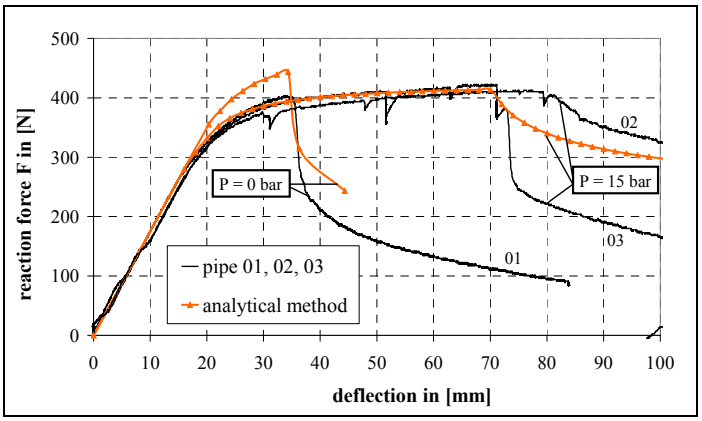

Figure 11: Comparison of the analytical calculation with the tests

In the case where P = 15 bar greater deflection and greater axial strains are reached before plastic shell buckling occurs. The region of postbuckling is reached with a slightly lower deflection in the analytical calculation, because according to Eq. 3 the value for the limit strain ε_{cr} at $\sigma_\Theta / \sigma_y = 0.45$ lies below both test values and is therefore on the safer side. The drop in the reaction force of pipe 2 (P = 15 bar) and analytical calculation is smoother than in the case of pipe 1 (P = 0 bar) due to the stabilizing effect of internal pressure. The decrease in reaction force of pipe 3 is more distinct than in the case of pipe 2, because for pipe 3 the scenario of a pressure reduction in the elasto-plastic range was investigated, and from u = 67.5 mm it was further deformed pressureless. For this reason the buckle failure of pipe 3 after approx. u = 70 mm resembles rather the test without internal pressure (pipe 1), characterized by a steep decline in force. The curves of pipe 2 and 3 show a better conformance with the analytical calculation in the prebuckling phase than the comparison for pipe 1, because the internal pressure causes a smoothing of the imperfections and thus the load-bearing capacity is not so markedly reduced. This elasto-plastic bearing behavior under internal pressure and imposed deformation could be verified by further tests (4 – 8) with a variation of internal pressure.

TRANSFER TO REAL BOUNDARY CONDITIONS

The experimental set-up for the test specimen is a closed system. An axial tensile stress acts at the pipe end caps resulting from internal pressure. The test specimen can be freely deformed in horizontal direction due to the boundary conditions at the pipe ends and thus follow a longitudinal change caused by bending without hindrance. The boundary conditions of a buried pipeline do not correspond with these test boundary conditions. A buried pipeline has basically no end caps and therefore also no longitudinal stresses resulting from internal pressure. Deflection forces associated with change in direction within bends of pipes are countered due to the embedding in the soil via friction over a short interval. Solely from the transverse contraction of the pipeline a resultant stress occurs in axial direction, which in the case of the material steel is equivalent to 30 % of the hoop stress caused by internal pressure.

The ends of the test specimens are horizontally non-braced. This means that the axial displacement of the test specimen resulting from the upthrust curvature can occur without hindrance. This is not possible in the case of a buried pipeline. It can be assumed that the pipeline is laid straight and cannot shift due to soil friction, in order to give way to a strain as a result of bending. This causes tensile stresses to occur in the longitudinal direction of the pipeline, which have a favourable influence on the bending in the load case in question here, since they significantly relieve the pipeline cross-section in the bending pressure range.

In order to be able to assign the findings gained in the tests to reality it is necessary to find a static system which reflects the real boundary conditions shown above with sufficient accuracy. Here the problem is posed that many soil mechanic parameters, which have an influence on the bedding conditions of the pipeline can either not be acquired or modelled within a Finite-Element-Analysis at all or only to a limited extent. Therefore the aim must be to develop a static system as simple as possible, which will manage with few and easily manageable parameters and nevertheless supply reliable results. A static system, which fulfils these boundary conditions, is represented in Fig. 12.

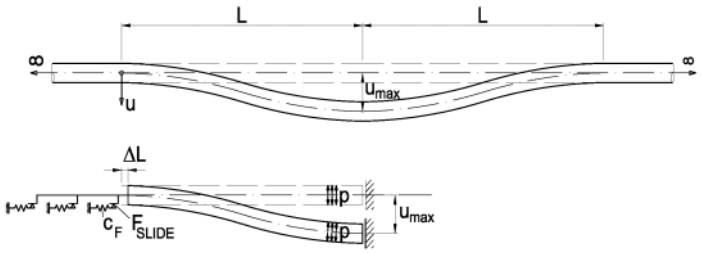

Figure 12: Real and idealised system

A symmetrical bending curve is presupposed, which permits the utilization of symmetrical conditions. In the area in which the settlement deformation occurs, no soil friction is stated as it is assumed that the pipeline moves with the surrounding soil. Beyond the settlement area axial springs are set. The rigidity (C_F) of the axial springs is derived from the bedding module of the soil surrounding the pipeline. For this a maximum spring force (F_{SLIDE}) can act, which is proportional to the shear stress acting between pipeline and soil. In this way a sliding friction is simulated. Conventional Finite-Element-Systems provide element types that are suitable for this. The imposed deformation is introduced by the half shells in the FE-model similarly as in the test on the tension side of the pipe cross-section. Fundamentally, the same problems exist numerically in the case of concentrated loads into shell structures as in reality. However, is described above, the decisive stresses occur in the bending compressive zone and the loading at the half shells is at a sufficient distance away, so that the local effects resulting from the points of load application are of subordinate significance.

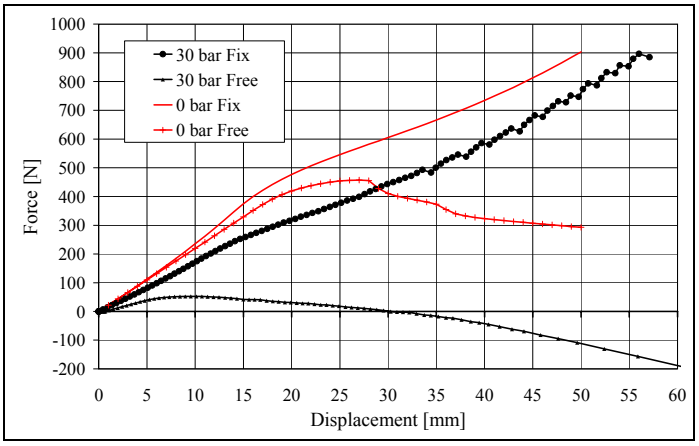

Figure 13: Comparison of different boundary conditions at different internal pressures

Fig. 13 shows the system behavior assuming extreme boundary conditions. In comparison to this the force-deformation diagram is assuming infinitely rigid axial bedding springs (Fix) and freely displaceable pipeline end (Free). A differentiation is made between an internal pressure of 0 bar and 30 bar. The ratio σ_Θ / σ_y for P = 30 bar is 0.9 (90 % of $f_{y,k}$). For the load case P = 0 bar and non-braced ends with a deflection of u = 28 mm an abrupt decrease in load can be observed, which points to the snapping of local buckling and a stability failure. For the load case P = 30 bar and free pipeline already at a considerably imposed deformation a drop in load down to the negative range can be observed. This can be explained by the fact that due to imposed deformation an arch develops, in which forces associated with change in direction begin to act. As soon as these forces reach a significant dimension, they push the pipeline in the direction of the imposed deformation and lead to a breakthrough and to a system collapse. In the graphs P = 0 bar and P = 30 bar for the systems with infinitely rigid springs it is evident that the deflection can be infinitely increased in principle, without resulting in a decrease in strength and thus to a system collapse. This can be explained by the fact that due to the hindrance of the axial displacement of the pipeline by the upthrust deformation a lengthening and a significant axial stress are produced, which lead to a stabilisation. It is immediately evident, that the static system „buried pipeline“ will move between these two extreme limits. A pipeline section under consideration will never be non-braced in axial direction, but nevertheless it cannot be basically assumed that the displacement will be prevented 100%. As an example, pipeline regions near bends or not ideally straight laid pipelines could be mentioned. An estimate of the spring strength via the above-mentioned bedding module parameter of the surrounding soil and maximum transferable shear stress between pipeline and soil permits a good calibration of the static system and so, too, a calculation of the pipeline systems stressed by settlement. Fig. 14 shows the result for P = 30 bar and soil friction. It can be seen that the assumption of a bedding rigidity (a pipeline buried in compressed sand was chosen) effectively prevents the breakthrough of the system.

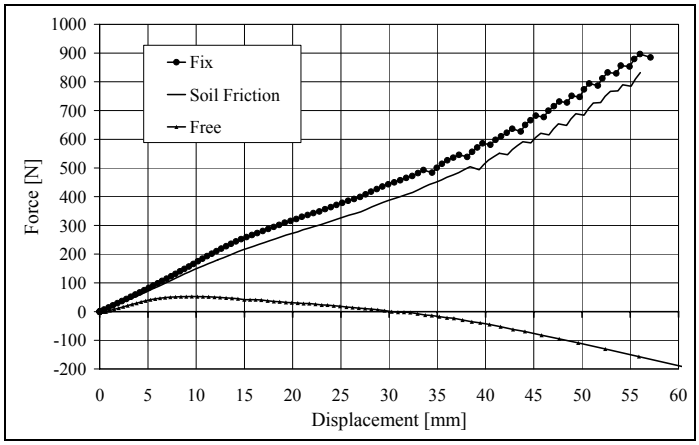

Figure 14: Comparison of different boundary conditions at P = 30 bar

LIMIT STRAIN FOR REAL APPLICATIONS

The tests have been carried out on the statically more sensitive system, caused by the chosen boundary conditions. As a result of the freely displaceable pipeline ends buckling occurs due to sufficiently large imposed deflection in the bending compressive zone and therefore to the collapse of the system. Because this system behavior can be excluded in reality, the test results for critical strain values represent a lower limit for the application for real design problems. The question of safety coefficients is not taken into account here. This aspect, however, can not be answered with a general validity because

there are great differences in the form of national regulations and in each case a suitable safety must be chosen.

It has to be remarked, that pipelines under thermal loading will behave different. Under sub-zero conditions, the soil surrounding the pipe freezes and soil friction will be reduced to almost zero. High temperature pipelines, which are anchored due to soil friction will be subjected to axial compression which may be lead to increasing curvature in settlement areas.

CONCLUSION

Experimental and numerical investigations from an ongoing research project are presented about steel pipes exposed to internal pressure and additional loads.

The investigations have shown that as far as the problem of the "Bending of a pipeline under internal pressure" is concerned this is not mainly a question of a stress problem but rather a problem of deformation capacity (e.g. buckling). The internal pressure has a supporting effect which significantly reduces the pipe's susceptibility to buckling.

It was achieved a good agreement between test results and numerical simulations. Even highly concentrated nonlinear states such as buckling patterns and various load histories were simulated correctly. Parallel to the numerical simulation it was possible to reproduce the bearing-behavior within the elasto-plastic range analytically adopting differential relationships. It was possible to formulate a general approach to the indication of critical limit strains based on these investigations.

The FE-Model calibrated to the tests was modified for the calculation of buried pipelines so that it was possible to take real boundary conditions into account. The axial bedding of the pipeline in the surrounding soil, which is decisive for the determination of strains in the case of settlement problems, could be simulated via spring-slide-elements, the rigidity parameter whereof being derived from the soil properties. This showed that the critical strains gained in the tests can be referred to as lower and therefore safe barrier for real applications.

It was the aim to formulate generally valid principles. For this reason the investigations were carried out on the basis of characteristic values and safety coefficients are not included. These are to be adapted to meet the national guidelines and applications for real design problems.

ACKNOWLEDGMENTS

The authors thank the German Federation of Industrial Cooperative Research Associations "Otto von Guericke" (AiF) for funding the research work within the program "Future Technologies for Small and Medium Companies" (ZUTECH).

REFERENCES

[1] ASME, 1998, "Boiler and Pressure Vessel Code (BPVC)", *ASME,* Pt III

[2] Bai, Y, 2003, "Marine structural design" *Elsevier,* Amsterdam

[3] DIN EN 1594, 2000, "Gas supply systems – Pipelines for maximum operating pressure over 16 bar – Functional requirements" Ref.-Nr. DIN EN 1594:2000-09

[4] Galambos, T. V., 1998, "Guide to stability design criteria for metal structures", *John Wiley & Sons,* 5th edition

[5] Gresnigt, A. M., 1986, "Plastic design of buried steel pipelines in settlement areas", *Heron,* Vol. 31 No. 4

[6] Hauch, S and Bai, Y, 1999, "Bending Moment Capacity of Pipes", *Proceedings of the 18th International Conference on Offshore Mechanics and Arctic Engineering,* OMAE, St Johns, Newfoundland Canada Paper No PL-99-5033

[7] Krysik, R, 1994, "Stability of steel truncated cone and cylindrical shells under axial compression and internal pressure", *"Stabilität stählerner Kegelstumpf- und Kreiszylinderschalen unter Axial- und Innendruck"*, *Dissertation* University of Essen, Germany

[8] Reddy, B. D., 1979, "An Experimental Study of the Plastic Buckling of Circular Cylinder in Pure Bending", *Int. J. Solid and Structures,* Vol. 15, pp. 669-683

[9] Zimmerman, T. J. E. and Stephens, M. J. and De Geer, D. D. and Chen, Q., 1995, "Compressive strain limit for buried pipelines", *Proceedings of the 14th International Conference on Offshore Mechanics and Arctic Engineering,* OMAE, Copenhagen, Vol. V – Pipeline Technology

